The Journal of Adhesion

ISSN: 0021-8464 (Print) 1545-5823 (Online) Journal homepage: www.tandfonline.com/journals/gadh20

Correlation between interlaminar shear strength of CFRP and joint strength of aluminium-CFRP hybrid joints

Shuang Wu, Alexander Delp, Jonathan Freund, Frank Walther, Jan Haubrich, Miriam Löbbecke & Thomas Tröster

To cite this article: Shuang Wu, Alexander Delp, Jonathan Freund, Frank Walther, Jan Haubrich, Miriam Löbbecke & Thomas Tröster (2025) Correlation between interlaminar shear strength of CFRP and joint strength of aluminium-CFRP hybrid joints, The Journal of Adhesion, 101:10, 1193-1218, DOI: 10.1080/00218464.2024.2439956

To link to this article: https://doi.org/10.1080/00218464.2024.2439956

Published online: 08 Jan 2025.

THE JOURNAL OF ADHESION
2025, VOL. 101, NO. 10, 1193–1218
https://doi.org/10.1080/00218464.2024.2439956

Taylor & Francis
Taylor & Francis Group

Correlation between interlaminar shear strength of CFRP and joint strength of aluminium-CFRP hybrid joints

Shuang Wu[a], Alexander Delp[b], Jonathan Freund[c], Frank Walther[b], Jan Haubrich[c], Miriam Löbbecke[c], and Thomas Tröster[a]

[a]Chair of Automotive Lightweight Design, Paderborn University, Paderborn, Germany; [b]Chair of Materials Test Engineering (WPT), TU Dortmund University, Dortmund, Germany; [c]German Aerospace Center (DLR), Institute of Materials Research, Cologne, Germany

ABSTRACT

Fibre-reinforced polymers are increasingly used due to their high specific strength, making them suitable for local sheet metal reinforcement. This allows improved overall mechanical properties with reduced wall thickness of the sheet metal part and, thus, lower weight of the components. One of the main focuses of research into such hybrid structures is on the adhesive properties and the respective failure behaviour of the interfaces. Generally, the failure behaviour under the influence of mechanical loads can be divided into adhesive, cohesive and mixed-mode failure. The correlation between observed failure behaviour and adhesion properties of the hybrid composite materials is analysed in detail in this work. The hybrid composite consists of an aluminium sheet of the alloy EN AW-6082 T6 and thermoset carbon fibre-reinforced plastic (CFRP) prepreg. The aluminium sheet was laser pretreated before hybrid production to improve the adhesion properties. The specimens studied were produced by the prepreg pressing process, in which the components are cured and joined simultaneously. The influences of the thickness of the CFRP part, the layup, the fibre orientation at the boundary layer, and the laser pretreatment parameters on the properties of the hybrid joints were investigated.

ARTICLE HISTORY
Received 23 July 2024
Accepted 25 November 2024

KEYWORDS
Prepreg pressing process; hybrid joints; laser surface pretreatment; intrinsic manufacturing; CFRP; aluminium; materials engineering

1. Introduction

Since transport is the second largest contributor to GHG emissions, developing innovative lightweight construction concepts in the automotive sector is essential for achieving climate neutrality in Europe and reducing Greenhouse Gas Emissions (GHG).[1] Various studies have investigated how emissions and energy consumption depend on vehicle design parameters such as rolling resistance, aerodynamic drag, and, most importantly, vehicle mass. It is already known that vehicle mass is a decisive factor in reducing fuel consumption and thus improving energy efficiency in developing new innovative

CONTACT Shuang Wu shuang.wu@upb.de Chair of Automotive Lightweight Design (LiA), Paderborn University, Mersinweg 7, Paderborn 33100, Germany

internal combustion engine vehicles (ICEVs). The same principle also applies to Battery Electric Vehicles (BEVs). Reducing the vehicle mass can either increase the electric range while maintaining the same energy storage or reduce the energy storage and, thus, the storage costs while maintaining the same range.[2] For example, depending on the vehicle model or the driving cycle, energy consumption could be reduced by 0.47–1.17 kWh/(100 km × 100 kg) for BEVs and by 0.1–0.6 l/(100 km × 100 kg) for ICEVs.[3,4] Although weight reduction can reduce the manufacturing and total costs of both ICEVs and BEVs, the study by Hofer et al.[5] showed that there is an optimum degree of weight reduction for reducing costs. Due to the high share of fuel consumption in the total costs, ICEVs show a higher sensitivity to weight reduction, so the optimal weight reduction for reducing manufacturing costs is 10% and for total costs, 28% (150.000 km driving distance) and 31% (300.000 km driving distance). In contrast, the optimal weight reduction of BEVs for reducing manufacturing costs is 24%, for total costs 28% (range 200 km) and 39% (400 km range).

A well-known approach for lightweight automotive construction is the multi-material design, in which Fibre-Reinforced Polymers (FRP) are combined with metallic materials.[6] The design allows the production of lightweight, load-bearing structures with high fatigue and impact resistance.[7,8] Furthermore, although the manufacturing process of FRP is more energy-intensive than metal production, the resulting weight reduction by applying FRP can reduce CO_2 emissions over the entire lifetime of the vehicle.[9] When using such hybrid structures, the joint strength at the interface plays a major role in transferring stresses between metal and FRP materials. A weak adhesion can lead to delamination of the interfaces and a reduction in the mechanical performance of metal-FRP hybrid components.[10] The joint strength can vary significantly depending on the applied joining technique and the surface pretreatment prior to joining. Conventional mechanical joining methods, such as riveting and bolting, can be applied to hybrid composites. However, it must be mentioned that mechanical joining often leads to damage to the joining partner and an increased risk of corrosion. In contrast, the adhesive joining of metals and FRP offers the advantage of a uniform stress distribution and enhanced fatigue strength. Moreover, enhanced corrosion properties and additional weight reduction can be achieved [11–13].

Surface pretreatments, such as sandblasting, anodising, or laser pretreatment of the metal adherent before bonding, can be advantageous for joint strength. One up-and-coming method, the pulsed laser pretreatment, is characterised by high precision, efficiency, environmental friendliness and simple implementation of industrial applications.[14] Various studies have shown that laser technology positively affects adhesion properties through surface enlargement and roughening. Voswinkel et al., for example, investigated the adhesion properties of steel-carbon fibre reinforced polymer (CFRP) hybrid

composites with laser-pretreated steel sheets.[14] The sheets were pretreated with a pulsed YVO_4 laser at different scanning speeds and pulse frequencies. The investigations proved that the joint strength increased almost linearly with the spot density. Slowing the scanning speed or increasing the frequency can increase the spot density. Compared to untreated specimens, the joint strength could be increased by 15% to 18%.

Similar to,[14] Freund et al. researched the influence of laser technology on the adhesion properties of bonded epoxy-aluminium joints. In this study, instead of a pulsed YVO4 laser, the Nd:YAG-Laser was used, and the laser pulse energy, frequency, laser spot overlap and number of scans were varied to investigate their influence on producing structured surface. The adhesion properties were examined with a single lap-shear test. In addition, half of the specimens aged in deionized water at 80°C for seven days to assess their ageing properties. The results indicated that the specimens with dense nanostructures and deep surface structures showed high shear strength and low loss in shear strength after ageing, which can be attributed to the high surface enlargements on the micro- and nanoscale. However, it was also concluded that these factors can be compensated by each other, as the specimens with lower microstructure depth and high micro- and nano-surface enlargement values can also achieve high shear strength.[15]

Akman et al. investigated the influence of laser-generated groove structures on the joint strength of Al/CFRP joints. The results showed that a deep groove structure created with a parameter set of 50 W laser power, 80 kHz frequency, and 800 mm/s scanning speed results in enhanced shear strength and mechanical interlocking. The higher the number of scans, the deeper the resulting groove structures. A maximum shear strength of 26.48 MPa was achieved.[16] In addition, the surface of FRP can also be pretreated using, for example, infrared (IR) or Ultraviolet (UV) laser to maximise the adhesion strength. However, the laser parameters, such as wavelength and energy input, should be carefully selected to avoid fibre damage or deterioration of the fibre-matrix adhesion.[17,18]

By co-curing metal and composite, the resin of the FRP serves directly as an adhesive that bonds the single components during forming. This substitutes further process steps. Such a process is often referred to as intrinsic manufacturing.[19] Our preliminary work investigated the intrinsic manufacturing of hybrid composites from laser-structured EN AW-6082 T6 aluminium sheet and CFRP using a prepreg pressing process without additional adhesives. The resulting laminate quality, shear strength and fracture surfaces were characterised, and suitable laser pretreatment and curing parameters (curing temperature, curing time, pressure) were determined. The results showed that all selected laser parameters (three combinations) can improve the shear strength. However, the laser parameter that produces lower structure depth and undercutting on the surface of the metal sheet shows a significantly lower improvement in shear strength with increased pressing pressure. One possible reason for this is the increased resin leakage at increased pressure. Additional tests were therefore carried out to

determine the fibre volume fraction at different pressures. The results showed that at a temperature of 150°C and a curing time of 20 min, the fibre volume fraction is the lowest at 43% and a pressing pressure of 0.3 MPa and increases to 47% at 0.5 MPa and 67% at 0.8 MPa, which indicates that the resin can be pressed out more at increased pressure.[20] During the pressing process, the resin system could be better trapped in the structure if the microstructure produced has a greater depth and more undercuts. In contrast, the resin system could not penetrate well into the microstructure with a shallow depth, which could lead to increased resin leakage at increased pressure and, thus, lower resin content at the interface. Since no other adhesives were used and the resin system serves directly as an adhesive, a low resin content can, therefore, lead to poor adhesion.

In the preliminary work, the fracture surfaces of the analysed specimens showed significant differences. The specimens with deep melt craters in the interface exhibited cohesive failure in the CFRP.[20] Cohesive failure indicates that the joint strength of the interface is higher than the inherent strength of the joining partners. As part of this work, extended investigations on the adhesion properties of EN AW 6082-T6-CFRP hybrid joints and pure CFRP laminates were carried out. The layer structure, the number of prepreg layers of the CFRP laminate, the fibre orientation at the boundary layer, and the laser scanning direction were varied to characterise their influence on the adhesion properties and failure behaviour. These tests allow conclusions about the effect of laser parameters on the adhesion properties and the failure behaviour. On the other hand, the relationship between the failure mechanisms of the hybrid joints and the interlaminar shear strength of the CFRP can be analysed.

2. Materials and methods

2.1. Materials

The hybrid joints investigated in this work consists of a laser-structured aluminium alloy EN AW-6082 T6 sheet and unidirectional carbon fibre epoxy prepreg SIGRAPREG®C U230–0/NF-E320/39% (SGL Carbon, Wiesbaden, Germany), the same as in the prior study.[20] In order to investigate the influence of the interlaminar shear strength of CFRP on the adhesion properties of the hybrid composite, pure CFRP laminates with the same prepreg systems were also produced.

2.2. Laser surface treatment

Prior to the pressing process, the surface of the aluminium sheet was pretreated with a pulsed Nd: YAG CL20 laser (Clean Lasersysteme GmbH, Herzogenrath, Germany) with a wavelength of 1064 nm and a spot diameter of 65 µm. The laser pretreatment was realised at the German Aerospace Centre (DLR) in Cologne.

Table 1 specifies the laser parameter used in this work. The laser spots overlap by 10% in the x and y directions, and the laser beam passes over the surface five times in the x direction and then changes to the next position in the y direction (Figure 1).

The preliminary work proved that cohesive failure in the CFRP occurs in hybrid specimens produced with the laser parameter set one (L1 in Table 1), which shows an average crater depth of 33 µm.[15,20] Therefore, the L1 parameter set is chosen for further investigations of the correlation between the interlaminar shear strength of CFRP and the shear strength of the hybrid composites.

In addition, the angle at which the laser interacts with the metal surface was varied, as a direction-dependent laser structure is generated at L1 (see Figure 2a). Scanning direction 1 (SD1) means the laser scanning direction is along the fibre direction of the first prepreg layer at the interface. In contrast, scanning direction 2 (SD2) is transverse to the fibre direction. The specimens were cut from the plates in a way that the fibre orientation is 0° (0°-specimens) or 90° (90°-specimens) to the load direction during the shear edge test (Figure 2b).

2.3. Specimen manufacturing using the prepreg pressing process

The previous study concluded that the specimens cured at a temperature of 150°C and a pressing pressure of 0.5 MPa for 20 minutes achieved high joint strength.[20] Therefore, the curing parameters were set accordingly and did not vary further for the specimens analysed in this work. The pressing process was

Table 1. Parameter of laser pretreatment on 2 mm EN AW-6082-T6 sheets.

Parameter	Frequency [kHz]	Power [W]	Overlap Laserspots [%]	Number of crossing
L1	60	20	10	5

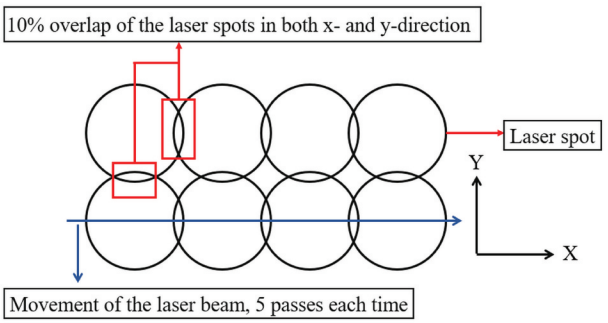

Figure 1. Illustration of the overlap of laser spots and the number of crossings.

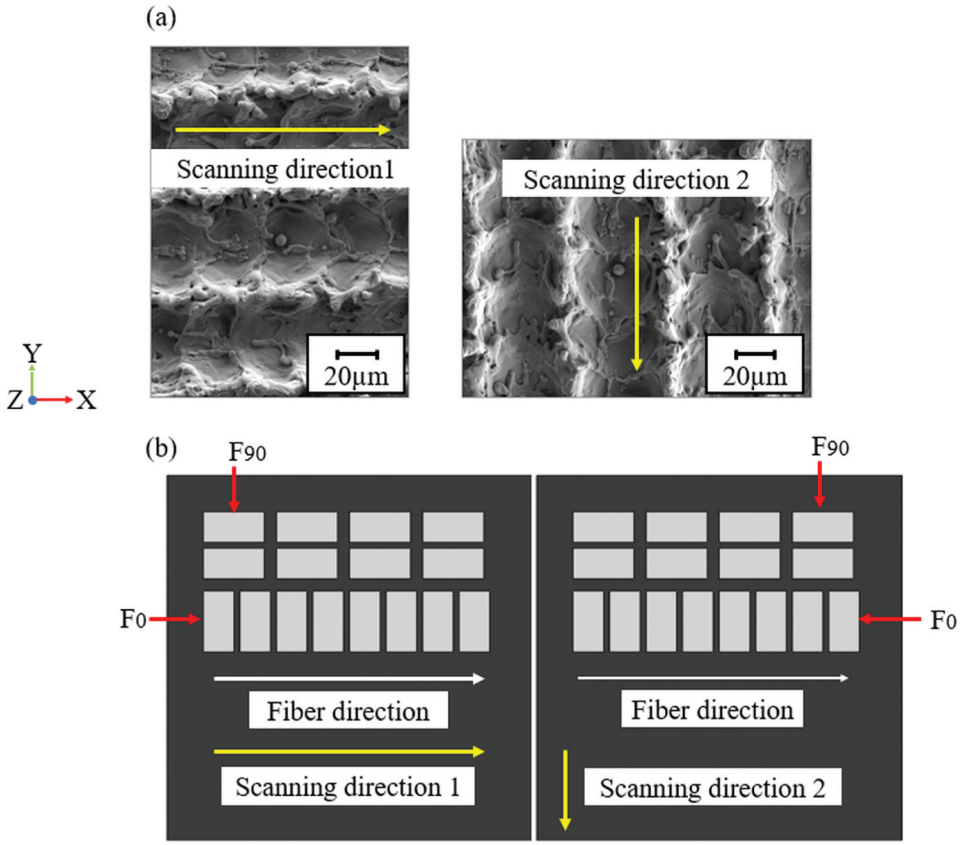

Figure 2. (a) Scanning electron microscope (SEM) recordings of the surface structure of laser parameter 1, (b) illustration of the scanning- and fibre direction, F_0 indicates the load direction for 0°-specimens and F_{90} for 90°-specimens during shear edge test.

realised with a PS200 laboratory press (VOGT Labormaschinen GmbH, Berlin, Germany). The number of prepreg layers and layer structures varied for both the hybrid and CFRP specimens (Table 2).

The unidirectional (UD in Table 2) and multiaxial layer structure (MA in Table 2) of hybrid specimens is shown in Figure 3 using the example of hybrid specimens with eight prepreg layers. For the CFRP specimens, the number of prepreg layers is selected so that the thickness after pressing and curing is as similar as possible to that of the hybrid specimens to achieve a similar load condition. Therefore, the fibre direction of CFRP specimens

Table 2. Layer structure and number of prepreg layers of hybrid- and CFRP specimens.

	Hybrid specimens		CFRP specimens	
Prepreg-layers	6	8	14	16
Layer structure	UD	UD MA	UD	UD MA

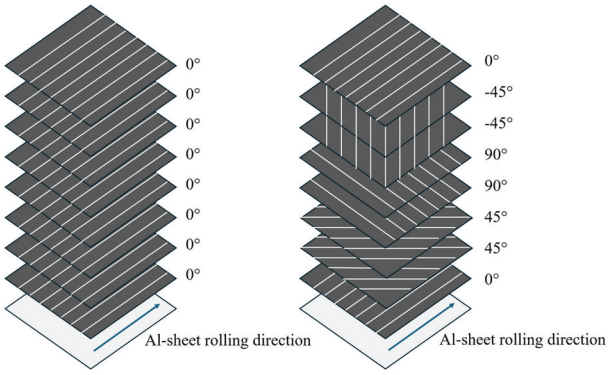

Figure 3. Illustration of the layer structure of hybrid specimens with eight prepreg layers.

with a unidirectional layer structure is all in 0° direction. In contrast, the multiaxial layer structure of CFRP is symmetrical [0°/45°/45°/90°/90°/-45°/-45°/0°]s.

Specimen plates measuring $150 \times 150\ mm^2$ were produced for mechanical testing. Before pressing, the 2 mm aluminium sheet was laser pretreated with the L1 parameter set. The CFRP prepreg was cut with a flat plotter (CAMTEC GmbH; Freilassing, Germany). The individual prepreg layers were stacked according to the layer structure. In the case of hybrid specimens, these stacked prepreg layers were placed on the laser-pretreated side of the aluminium sheet. A pressing tool was installed in the press and preheated to 150°C by the heating plates of the press (Figure 4). Then, the prepared material stack is placed in the tool cavity, and the pressing process begins. As soon as the pressure of 0.5 MPa is reached, the press switches to force control mode to maintain the pressure during the curing process. After the set pressing time of 20 minutes, the press opens automatically, and the specimen plates can be removed. An additional post-curing step was carried out on all pressed specimen plates in the oven at 180°C for 30 minutes.

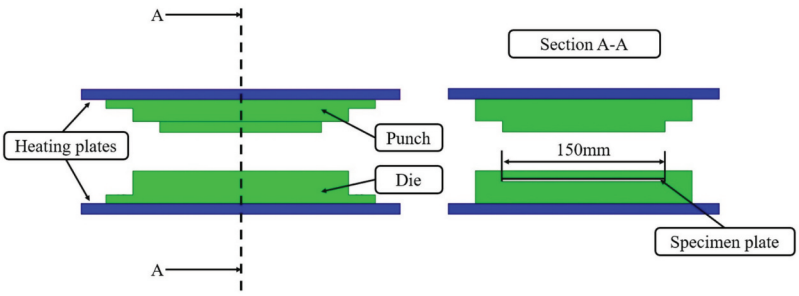

Figure 4. Pressing tool for specimen production, installed inside laboratory press and connected to heating plates.

2.4. Shear edge test

The shear edge test characterised the adhesion properties of the pure CFRP and hybrid specimens. Compared to tensile shear or short beam tests, this method has the advantages of simple sample preparation and more uniform stress distribution.[21] The device shown in Figure 5 is installed in a universal testing machine, Criterion 45 (MTS Systems GmbH, Berlin, Germany), with a load cell capacity of 100 kN. The test speed was set to 5 mm/min.

The specimens are extracted from the specimen plates by waterjet cutting. The thickness of the hybrid specimens is the sum of the thickness of the aluminium sheet ($t_{Al} = 2$ mm) and the CFRP (approx. 3.5 mm for six-layer prepregs, $t_{Hybrid,\ six\text{-}layer} = 3.5$ mm; and 4 mm for eight-layer, $t_{Hybrid,\ eight\text{-}layer} = 4$ mm; after pressing, see Figure 6).

During testing, the aluminium side with a thickness of 2 mm is clamped in the specimen holder (see Figure 5a,b). The shear edge (see Figure 5a) subsequently shears off the CFRP component, whose thickness is 1.5 mm for six-layer prepregs and 2 mm for eight-layer prepregs (see Figure 6). For the pure CFRP specimens, one part of the CFRP, $t = 2$ mm, the same as the aluminium sheet, is clamped in the test fixture. The other part is sheared off (Figure 5b). The shear strength is calculated by dividing the maximum force (F) recorded during the test by the actual interface area (b for length, h for height, Figure 6), measured using a calliper gauge before testing.

$$\tau = \frac{F}{b \times h} \qquad \text{(Eq.1)}$$

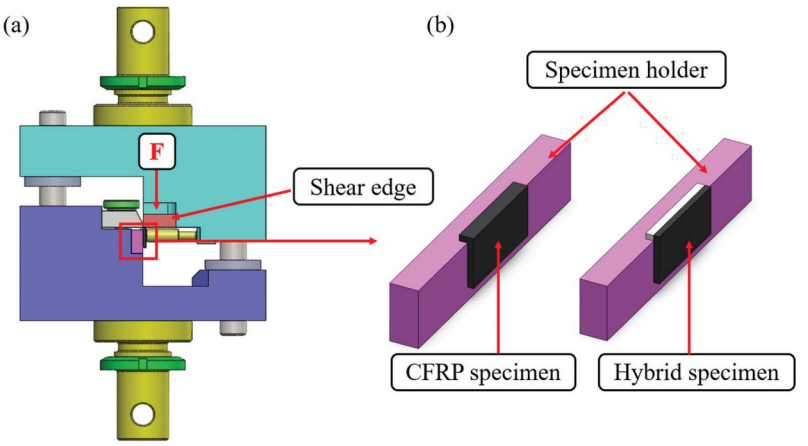

Figure 5. (a) Illustration of the device for shear edge test, (b) specimen clamping for hybrid and CFRP specimens.

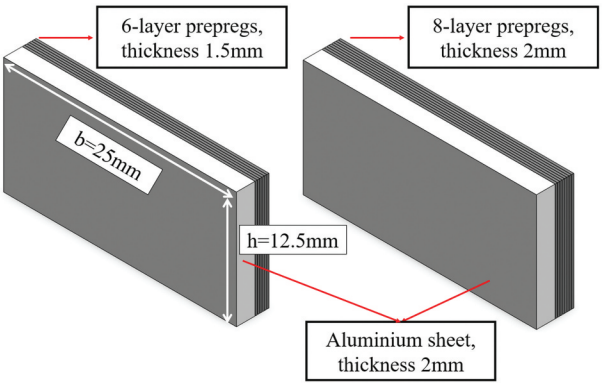

Figure 6. Illustration of the dimension of hybrid specimens with six and eight prepreg layers after pressing.

3. Results and discussion

3.1. Shear edge test results of hybrid and CFRP specimens with unidirectional layer structure

3.1.1. Hybrid specimens

In the first step, the influence of the thickness of the CFRP laminate on the joint strength of the hybrid specimens, in which the layer structure is unidirectional (UD), was investigated. Figure 7 shows the results of the EN AW-6082 T6/CFRP hybrid specimens. The names of the tested groups are listed in the order of scanning direction, number of prepreg layers, and layer structure. Thus, the test group SD1_6_UD indicates that the specimens were pretreated with SD1 and consisted of six unidirectional prepreg layers. 0° on the X-axis means that the direction of force application is in the fibre direction and 90° transverse to the fibre direction.

The resulting shear strengths are maximum when the force is applied in the fibre direction for each test group. The reason for this is assumed to be the higher stiffness of the carbon fibres in the load direction, which leads to an improved load introduction to the boundary layers[22–24] Thus, a more homogeneous stress distribution can be achieved in both the adhesive and the composites due to the stiffer 0°-fibres.[25] The study from Kowatz et al. shows similar results: the shear strength of steel/CFRP hybrid composites decreases with increasing fibre angle to the load direction.[26]

Figure 8 shows the representative stress-displacement curves of the 90°- and 0°-specimens of SD1_8_UD. It can also be seen that the force increases more steeply with 0°-specimens. Furthermore, the specimens exhibit an impact-like failure compared to the 90°-specimens, which can also be attributed to the stiff 0° fibres. Since the fibres, in this case, mainly bear the load.

During the experimental tests, five samples were tested per test group. Thus, it is difficult to tell from Figure 7 alone whether one test group is

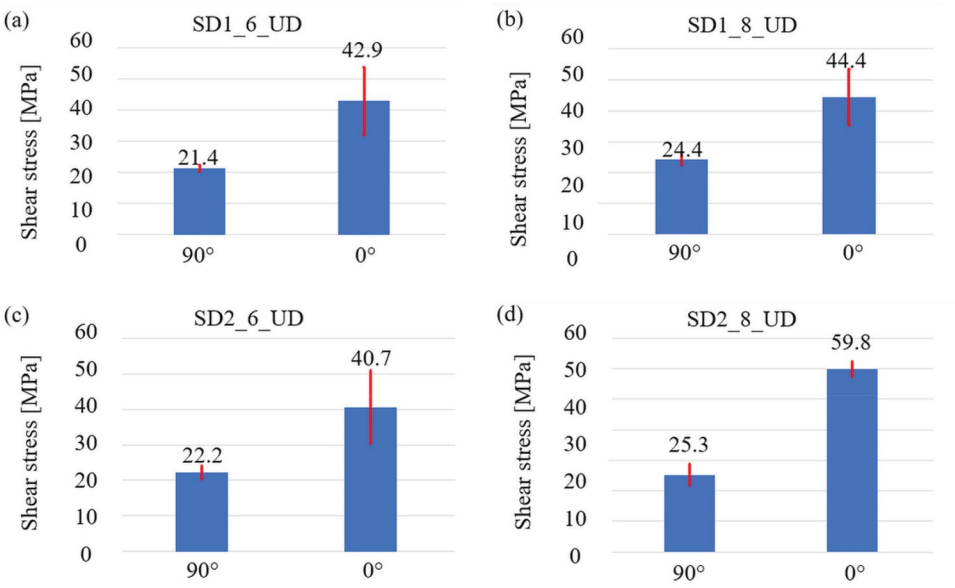

Figure 7. Shear edge test results of hybrid specimens with unidirectional layer structure and different numbers of prepreg layers, (a) and (b) SD1; (c) and (d) SD2.

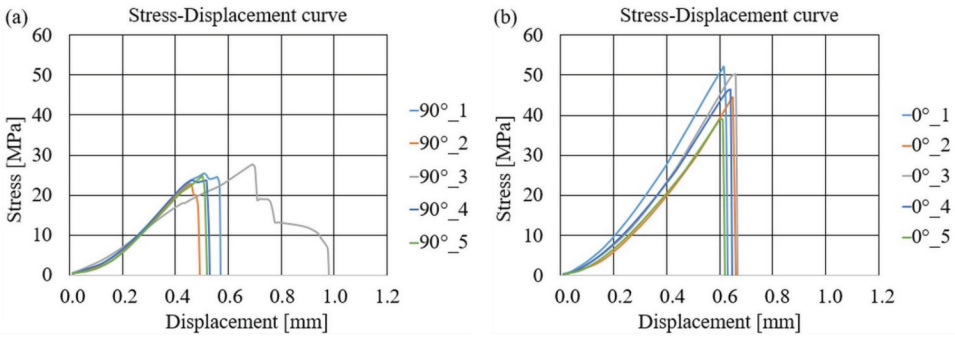

Figure 8. Representative stress-displacement curves of the shear edge test, results of (a) 90°- and (b) 0°-specimens of SD1_8_UD.

better than the other, although they sometimes show higher shear strength, e.g. the 0°-specimens of SD1_6_UD and SD1_8_UD. For this reason, the Analysis of Variance (ANOVA) method was used to analyse the results in a statistically reliable manner. This could ensure whether the determined shear strength differs statistically significantly between the tested groups for different parameters such as scanning direction and number of prepreg layers. A null hypothesis is defined for each analysis, and a P-value is calculated. In the context of this work, the null hypothesis is that the average shear strength determined is the same for the test groups examined. It is defined as follows: If a calculated P-value is less than 0.05, the results

of the two test groups differ statistically significantly, and the null hypothesis can be rejected.[27]

3.1.1.1. Number of prepreg layers. The ANOVA analysis shows that the determined shear strength depends on the number of prepreg layers of the CFRP laminate. When the number of prepreg layers is changed, significant differences in the resulting shear strengths can be assumed. For SD1, the shear strength (Figure 7a,b) determined for 90°-specimens is statistically higher with 8-layer prepregs (24.4 MPa) than with 6-layer prepregs (21.4 MPa).

The ANOVA input and output data are listed in Table 3. As described, the factor is the number of prepreg layers in the hybrid specimens, and there are two groups, one with six prepreg layers and the other with eight. In the ANOVA output table, the between-group sum of squares measures the variation in the data, which can be explained by the differences between groups. In contrast, the within-group sum of squares measures the variability in each test group. The F value is calculated by dividing the between-group sum of squares by the within-group sum of squares. The higher the F value, the more likely the differences in the data are due to group differences.[27] Another important value from the ANOVA output is the significance value (P-value), which in this analysis is 0.14, below 0.05. Therefore, there is a statistically significant difference in the determined shear strength between these two tested groups.

Figure 9 shows the boundary layer for SD1. It can be seen that the laser structure (in the X-direction) at SD1 is always perpendicular to the fibre direction (in the Z-direction). During the pressing process, individual fibres can be pressed into the laser structure so that a mechanical interlocking effect can be formed at the interface, positively affecting the joint strength. However, a notch effect along the load direction near the interface could also be generated due to the undercut for 90°-specimens, leading to stress concentration (Figure 9). By increasing the number of prepreg layers from six to eight, the CFRP part becomes thicker and stiffer, affecting the joint strength of the hybrid specimens.[28] Thus, the increased CFRP part stiffness enables a stronger connection, and the force can be better transferred despite the notch effect in the laminate.[29,30] Nevertheless, the joint strength at the interface is still higher than the interlaminar shear strength of the CFRP part, resulting in a cohesive failure near the interface. (Figure 10b)

Table 3. Input and output table of ANOVA for the unidirectional hybrid 90°-specimens with six and eight prepreg layers at SD1.

	ANOVA input	
Factor	Group	
Number of prepreg layers	Group 1	6 layers
	Group 2	8 layers

ANOVA output					
Factor	Sum of squares	df	Mean square	F	P-value
Between groups	24.758	1	24.758	9.378	0.14
Within groups	23.76	9	2.64		

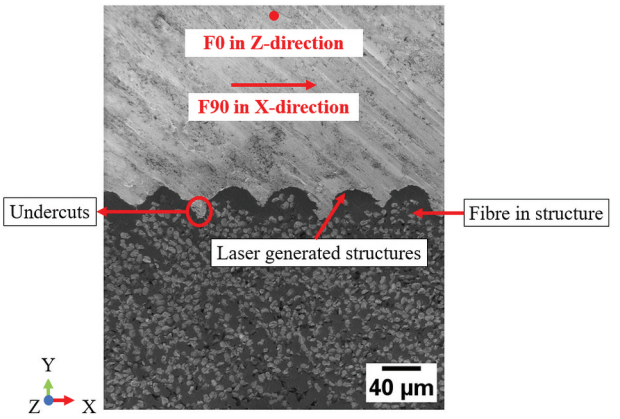

Figure 9. Cross-section SEM image of the boundary layer at SD1 and illustration of the force direction, F_0 for the 0°- and F_{90} for the 90°-specimens.

In contrast, the 0°-specimens do not show any significant differences by increasing the prepreg layers between the determined shear strength from a statistical point of view. The ANOVA output shows a P-value of 0.811 (Table 4), greater than 0.05.

One possible reason for this could be that no undercuts are generated in the direction of the force (F_0 in Figure 9), so no notch effect near the interface occurs as with the 90°-specimens. In this case, the carbon fibres close to the interface, which have a high stiffness along the loading direction, carry and transfer the shear stress until the specimens fail. Therefore, it is assumed that the laminate thickness no longer significantly influences the determined shear strength as in the 90°-specimens. However, the joint strength at the interface is higher due to the mechanical locking effect, leading to an early cohesive failure of the CFRP part near the interface (Figure 10a). Thus, the determined shear strength for both test groups is not the real shear strength at the interface but the interlaminar shear strength of the CFRP part. This is why the ANOVA output shows no significant differences between the test groups of the 0° specimens.

Specimens pretreated in scanning direction 2 (SD2), however, show an inverse phenomenon: the increased number of prepreg layers significantly increases the determined shear strength in 0°-specimens (59.8 MPa at eight layers and 40.7 MPa at six layers, (Figure 7c,d).

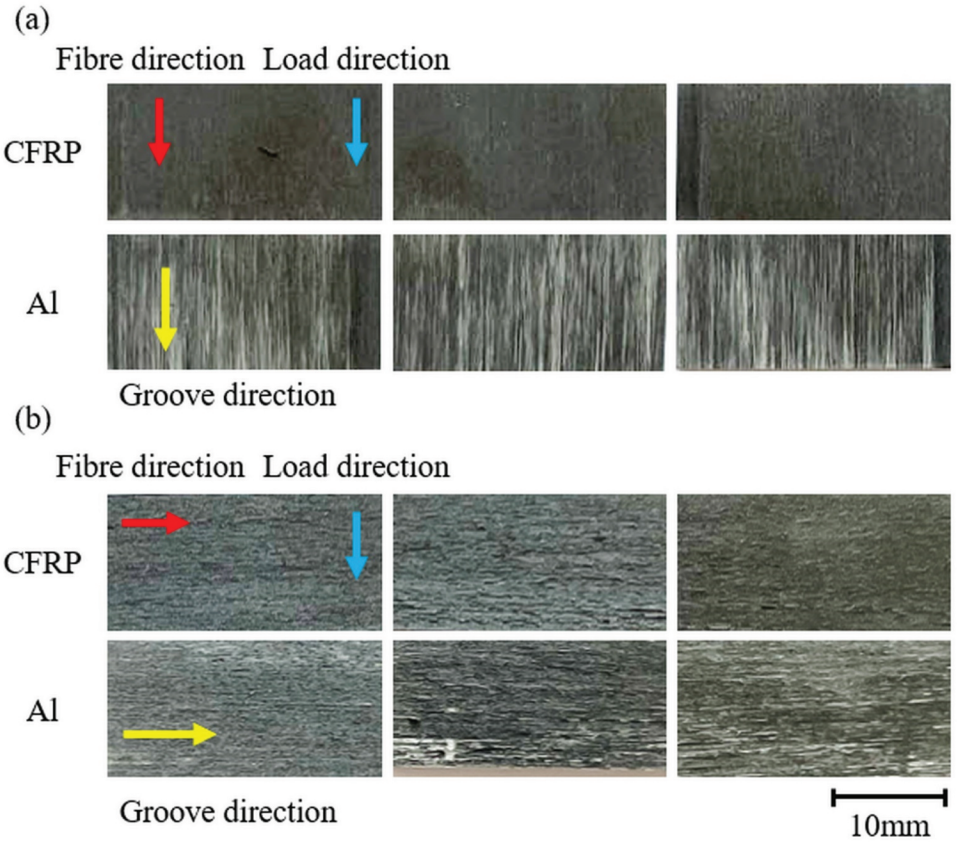

Figure 10. Fracture surfaces of (a) 0°- and (b) 90°-specimens of SD1_8_UD with the illustration of fibre direction of the first prepreg layer, load direction, and groove direction on the aluminium surface.

Table 4. Output table of ANOVA for the unidirectional hybrid 0°-specimens with six and eight prepreg layers at SD1.

ANOVA output					
Factor	Sum of squares	df	Mean square	F	P-value
Between groups	5.914	1	5.914	0.61	0,811
Within groups	873.391	9	97.043		

As visible in Figure 11, the laser pretreatment in SD2 leads to the direction of the laser structure (in the X-direction) along the fibre direction (also in the X-direction). In addition, unlike SD1, no fibres are pressed into the laser structure, only the epoxy resin. Therefore, for 0°-specimens, the increased thickness and stiffness of the CFRP part, as stated before, can allow the force to be better transmitted through the 0°-fibres to the interface. As a result, earlier failure in the CFRP part can be avoided. Thus, 0°-specimens with eight prepreg layers exhibit mainly adhesive failure at the interface instead of in the CFRP laminate (Figure 12b). In contrast, almost all specimens with six

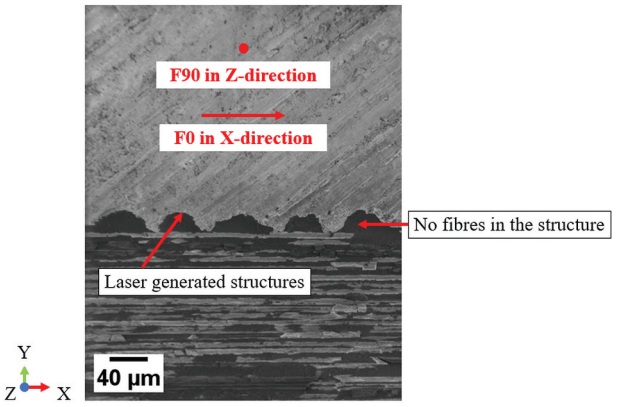

Figure 11. Cross-section SEM image of the boundary layer at SD2 and illustration of the load direction, F_0 for the 0°- and F_{90} for the 90°-specimens.

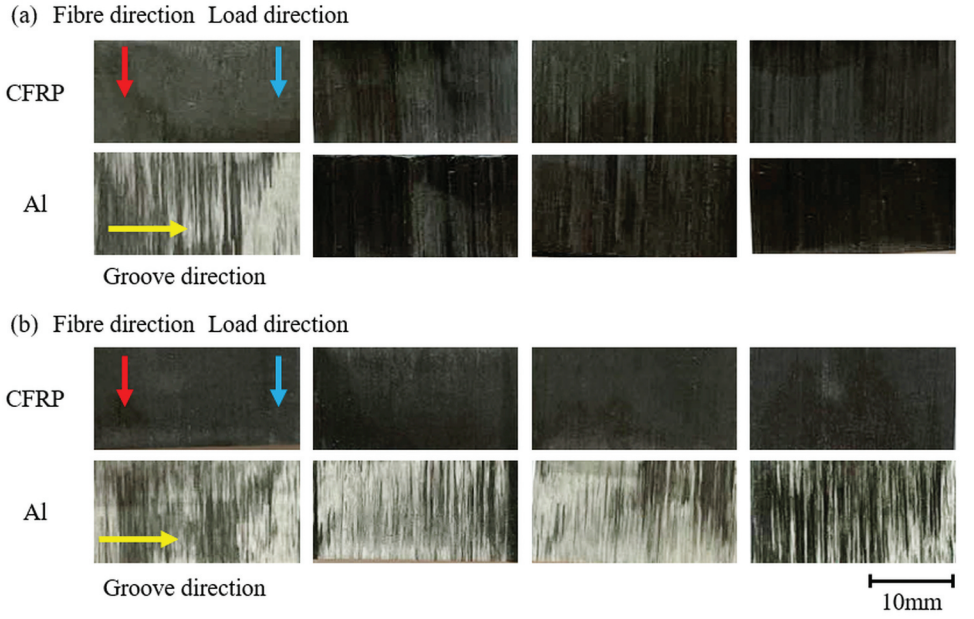

Figure 12. Fracture surfaces of the 0°-specimens of (a) SD2_6_UD and (b) SD2_8_UD with the illustration of fibre direction of the first prepreg layer, load direction and groove direction on the aluminium surface.

prepreg layers exhibit cohesive failure in the CFRP part (Figure 12a) since no aluminium surface was visible compared to the fracture surface of the 0°-specimens of SD2_8_UD. Thus, it can be deduced that the 6-layer specimens fail earlier in the laminate than at the boundary layer due to the lower stiffness of the CFRP part, which causes a comparatively lower average shear strength.

For 90°-specimens at SD2, ANOVA results show that increased prepreg layers do not enhance the determined shear strength. Since no fibres are

pressed into the laser structure (Figure 11) like the specimens at SD1 and the fibres have a lower stiffness in the transverse direction, the epoxy layer at the interface of 90°-specimens will bear and transfer the applied loads until the maximum load-bearing stress in the interface surface is reached. Therefore, it is assumed that the increased stiffness of the CFRP part does not significantly affect the joint strength at the boundary layer in this case.

3.1.1.2. Scanning direction. The ANOVA analysis showed that, only for the 0°-specimens with eight prepreg layers, there is a significant difference in the shear strength of specimens with different scanning directions (SD1 and SD2), with the shear strength at SD2 (59.8 MPa) being higher than that at SD1 (44.4 MPa) (see Figure 7b,d). Although the direction of force application is in the fibre direction for both SD1 and SD2 in the 0°-specimens, more fibres or epoxy resin could always be pressed into the groove structure at SD1, which can lead to better mechanical interlocking. This can enhance the joint strength of the interface so that failure occurs in the CFRP laminate. As a result, the CFRP laminate sometimes fails rather than the adhesion at the boundary layer, leading to increased cohesive failure (Figure 10a). Therefore, only a lower estimate for the shear strength can be found, which is not the true joint strength of the boundary layer. In contrast, the 0°-specimens with 8-layer prepregs pretreated in SD2 show reduced CFRP residues on the fracture surface (Figure 12b) and achieved higher shear strength. This indicates that the specimens fail at the boundary layer instead of in the CFRP laminate.

However, the determined shear strength does not directly indicate that SD2 can improve the joint strength of the hybrid composites better than SD1. On the contrary, the hybrid specimens with SD1 usually fail cohesively, which means that the joint strength at the boundary layer is stronger than the cohesive force in the CFRP.[31] Therefore, to prove this statement, it is necessary to investigate the interlaminar shear strength of the CFRP laminate to analyse the relationship between the joint strength and the failure mechanisms of the hybrid specimens.

3.1.2. CFRP specimens

The number of prepreg layers for pure CFRP specimens was selected and calculated based on the thickness of the hybrid specimens so that the thickness of the pure CFRP specimens was as close as possible to that of the hybrid specimen. (see Figure 13; the thickness of CFRP specimens with 14 prepreg layers and 16 layers is the same as the thickness of hybrid specimens with six and eight prepreg layers)

Unfortunately, the specimens in which the force direction is transverse to the fibre direction (90°-specimens) failed just below the point of application of the force (Figure 14a), which can be attributed to the lower stiffness of the 90°-

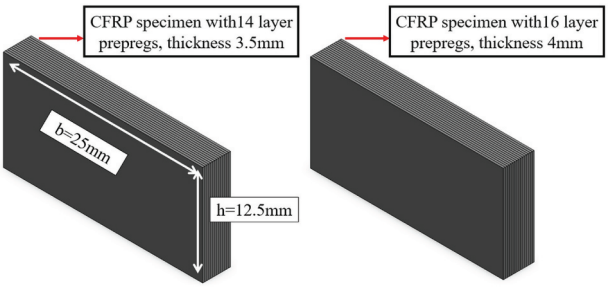

Figure 13. Illustration of the dimension of CFRP specimens with 14 and 16 prepreg layers after pressing.

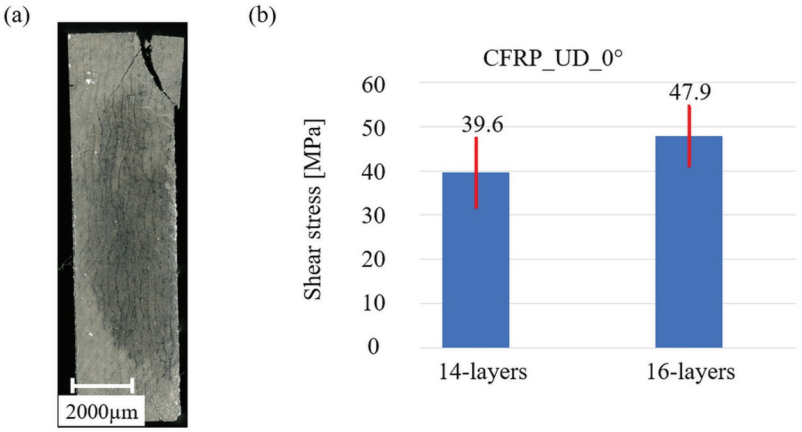

Figure 14. (a) Light microscope image of a failed CFRP 90°-specimen (b) shear edge test results of CFRP specimens with unidirectional layer structure and different numbers of prepreg layers, only 0°-specimens tested.

fibres. Therefore, they cannot be considered for comparison with hybrid joints since the failure mode was different. In contrast, the 0°-specimens (force direction in the fibre direction) failed between the prepreg layers. The results of shear edge tests are shown in Figure 14b.

The shear edge test results were analysed using the ANOVA method, which shows a P-value of 0.11, greater than 0.05 (Table 5). This means there are no significant differences in the determined shear strength between the two test groups from a statistical point of view. This could be expected because the same process conditions were used for all CFRP specimens with six and eight

Table 5. Output table of ANOVA for the CFRP 0°-specimens with 14 and 16 prepreg layers.

ANOVA output					
Factor	Sum of squares	df	Mean square	F	P-value
Between groups	170.597	1	170.597	3.2	0,111
Within groups	426.495	8	53.312		

prepreg layers. Therefore, their interlaminar shear strength should not differ significantly from each other.

3.1.3. Comparison of CFRP- and hybrid specimens

The determined shear strength of 6-layer hybrid 0°-specimens, both SD1 and SD2 (SD1_6_UD and SD2_6_UD), is only slightly higher than that of 14-layer CFRP specimens (Figures 7 and 14b). ANOVA analysis resulted in a P-value of 0.862, which is greater than 0.05 and indicates no significant differences in the shear strength between the hybrid- and the CFRP specimens. The fracture surfaces of the hybrid specimens (Figures 12a and 15) show that, except for one specimen of SD2, the hybrid specimens exhibit mostly cohesive failure in the CFRP laminate. This is also why ANOVA shows no significant differences in the determined shear strength between the hybrid and CFRP specimens. Therefore, it can be concluded that the interlaminar shear strength of the CFRP part is fully utilized, and the joint strength at the interface of the hybrid specimens is higher than that.

For 8-layer hybrid 0°-specimens, the average shear stress at SD2 ($\tau = 59.80$ MPa, Figure 7d) is significantly higher than that of the 16-layer CFRP specimens ($\tau = 47.90$ MPa, Figure 14b), indicated by a P-value of 0.008 in the ANOVA analysis. In contrast, no significant differences can be seen for SD1 specimens. As shown in Figure 12b, the fracture surfaces of the hybrid 0°-specimens with eight prepreg layers at SD2 also show a more pronounced adhesive failure at the interface than six prepreg layers. Therefore, the specimens fail mainly due to failure at the interface, and a higher shear strength can be achieved.

Compared to SD2 with eight prepreg layers (Figure 12b), more CFRP residues can be seen on the fracture surfaces of the 8-layer hybrid 0°-specimens with SD1 (Figure 16), which indicates that the joint strength of the interface is higher than the interlaminar shear strength of the CFRP laminate and the specimens fail partly in the CFRP laminate. On the other hand, although there are still CFRP residues on the fracture surface at SD1, the

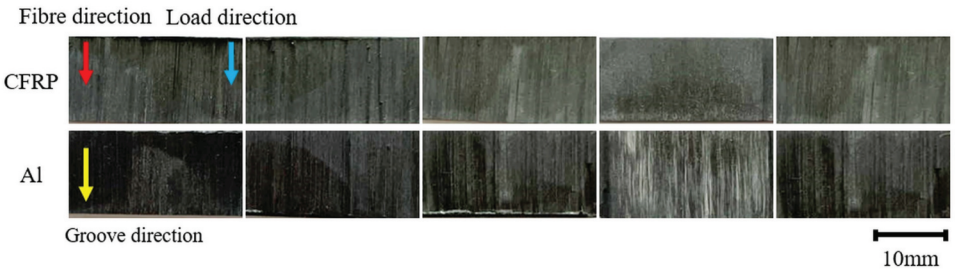

Figure 15. Fracture surfaces of 0°-specimens of SD1_6_UD with the illustration of fibre direction of the first prepreg layer, load direction, and groove direction on the aluminium surface.

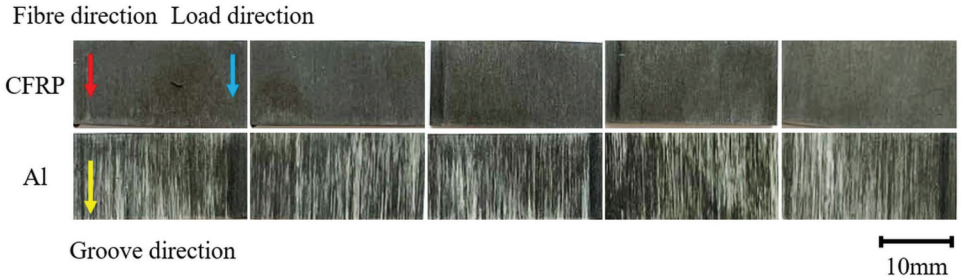

Figure 16. Fracture surfaces of 0°-specimens of SD1_8_UD with the illustration of fibre direction of the first prepreg layer, load direction, and groove direction on the aluminium surface.

Table 6. Summary of the failure mode of the various hybrid specimens and comparison of their shear strength with CFRP specimens.

Hybrid specimens	Failure mode	Comparison with CFRP specimens
SD1_6_UD_0	cohesive	No significant differences
SD2_6_UD_0	cohesive	No significant differences
SD1_8_UD_0	cohesive	No significant differences
SD2_8_UD_0	adhesive	Significantly higher than CFRP specimens

8-layer hybrid 0°-specimens exhibit already more pronounced adhesive failure compared to the 6-layer hybrid 0°-specimens (Figures 15 and 16), which indicates that the increased stiffness of CFRP part enables better load transfer to the boundary layer. However, the cohesive force in the CFRP laminate is still lower than the joint strength at the interface. Thus, the specimens fail when the interlaminar shear strength of the CFRP is reached. That is also why the ANOVA results show that the determined shear strength between CFRP and hybrid specimens does not differ significantly.

Table 6 summarises again the failure mode of the hybrid specimens with different scanning directions and prepreg layers. Overall, the comparison with the results of CFRP specimens confirms that the stiffness of the CFRP laminate enhances as the number of prepreg layers increases, allowing the force to be better transferred to the boundary layer. As a result, early cohesive failure in the CFRP laminate can be avoided, and higher shear strength can be achieved (e.g. SD2_8_UD_0 in Table 6).

3.2. Shear edge test results of hybrid and CFRP specimens with multiaxial layer structure

3.2.1. Hybrid specimens

The next step was to vary the layer structure of the CFRP laminate to investigate its influence on the joint strength of the hybrid specimens. Since the specimens showed improved shear strength with increased prepreg layers, only 8-layer hybrid and 16-layer CFRP specimens were produced. All hybrid

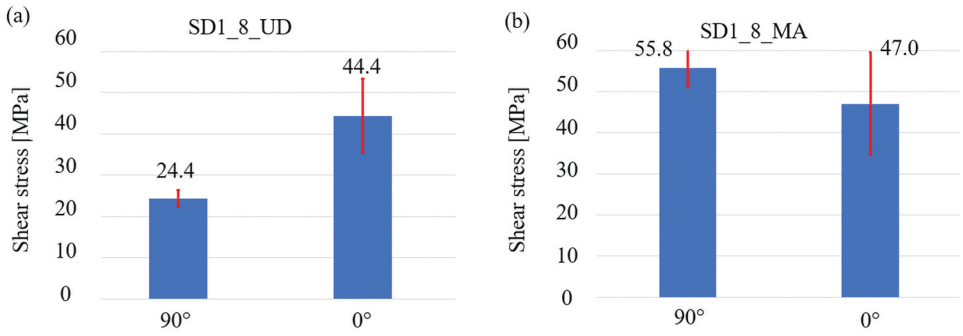

Figure 17. Shear edge test results of hybrid specimens with eight prepreg layers, (a) unidirectional layer structure, UD (b) multiaxial layer structure, MA.

specimens were pretreated with the laser scanning direction 1 (SD1_8_MA in Figure 17b).

The diagram above (Figure 17a,b) compares the shear edge test results of hybrid specimens with unidirectional and multiaxial layer structures. Although the 90°-specimens here still show a large proportion of cohesive failure with multiaxial layer structure (Figure 18b), which means that the specimens failed not at the boundary layer, the determined shear strength of 90°-specimens increases with multiaxial layer structure. It can be concluded that the multiaxial layer structure can increase the stiffness of the CFRP laminate, leading to a better load transmission compared to the unidirectional

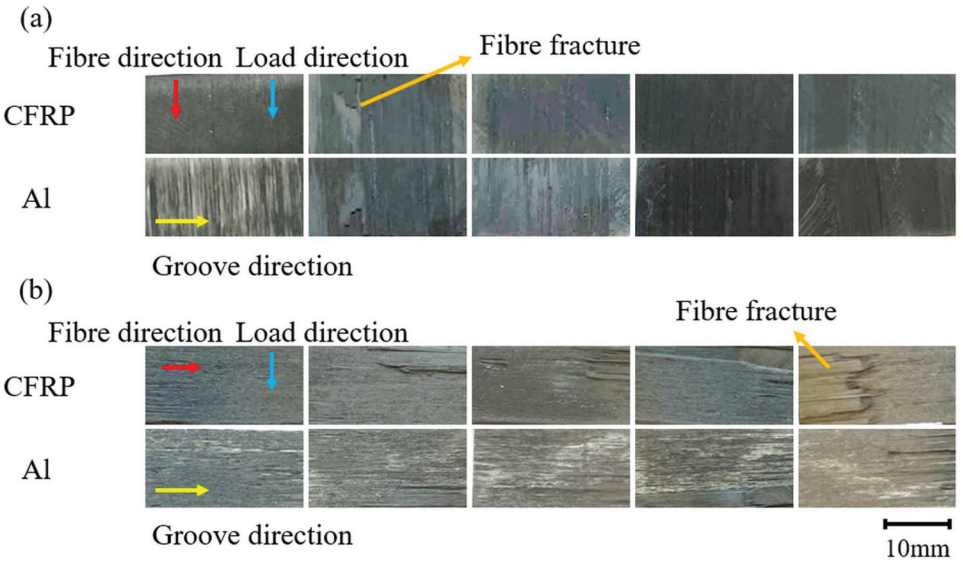

Figure 18. Fracture surfaces of (a) 0°- and (b) 90°-specimens of SD1_8_MA with the illustration of fibre direction of the first prepreg layer, load direction, and groove direction on the aluminium surface.

90°-specimens, and thus, higher shear strength was achieved. However, the joint strength at the interface is still higher than the shear strength in the laminate, so the specimens still exhibit a large proportion of cohesive failure in the laminate. In contrast, the shear stress of 0°-specimens does not increase significantly (Figure 17a,b), confirmed by the ANOVA analysis (P-Value 0.695). It is assumed that the layer structure has a negligible influence if the direction of force application is equal to the fibre direction.

Moreover, unlike the specimens with unidirectional layer structure, the ANOVA results showed that the determined shear strength of the 0°- and 90°- specimens did not show significant differences with multiaxial layer structure (P-Value 0.176). It is assumed that specimens with a multiaxial layer structure with identical stiffness in both directions are less sensitive to the fibre orientation in the boundary layer. Furthermore, compared to the fracture surface of the UD specimens, in addition to the delamination between the prepreg layers, fibre fractures of individual fibre bundles can be seen (Figure 18). This phenomenon can probably be attributed to the changing fibre direction (45°) of the neighbouring prepreg layer. The change in fibre direction also results in an abrupt change in stiffness in the CFRP laminate, which causes load redistribution and a weak point (Figure 19). For this reason, the formation of a crack can be favoured, which leads to a fibre fracture.[32] On the other hand, due to the more complex crack propagation, a higher shear strength can also be achieved compared to UD specimens.[33,34]

3.2.2. CFRP-specimens

The layer structure of the CFRP specimens is symmetrical [0°/45°/45°/90°/90°/-45°/-45°/0°]s, resulting in a thickness of $t \approx 4$ mm, which corresponds to the thickness of the hybrid specimens. The symmetry plane of the CFRP laminate is the plane through which the shear edge shears off. Figure 20a shows the average shear strength determined for 0° and 90°-CFRP specimens, and Figure 20b shows the 95% confidence interval of both test groups. The 95% confidence interval means that the average values determined for the two groups lie within this range with 95% probability.[27] In addition, as already mentioned, the multiaxial layer structure can increase the stiffness of the CFRP component. Therefore, CFRP 90°-specimens with a multiaxial layer structure

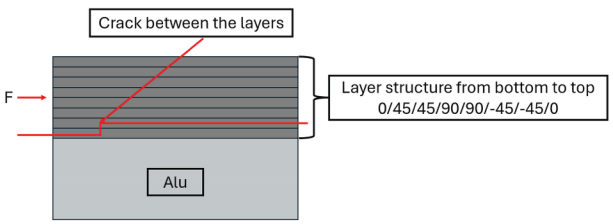

Figure 19. Illustration of the crack path of specimens from test group SD1_8_MA.

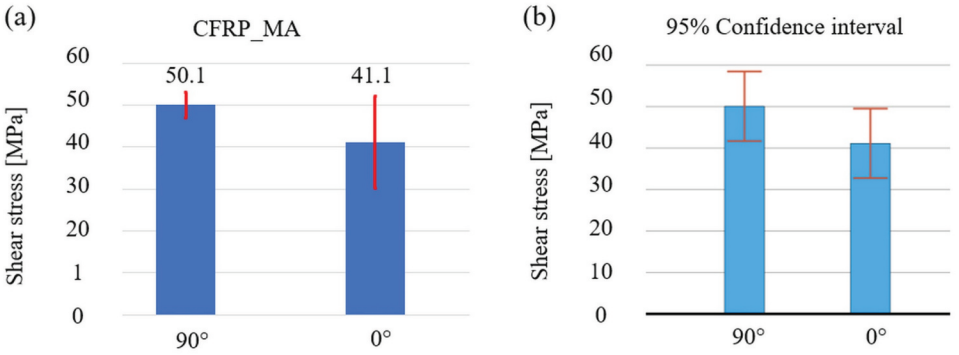

Figure 20. (a) Shear edge test results of CFRP specimens with multiaxial layer structure, (b) illustration of the confidence interval of the tested groups.

can provide valid results since they do not break at the point of force application, as with the unidirectional layer structure.

Although the 90°-specimens appear to reach higher shear stress (Figure 20a), a P-value of 0.12 (greater than 0.005) was calculated in the ANOVA analysis. In addition, it can be seen from Figure 20b that the 95% confidence interval of the two test groups overlaps. Thus, significant differences in the determined shear strength between the 0°- and 90°-CFRP specimens cannot be assumed.

One possible reason for this, as with the hybrid specimens (see 3.2.1), is that the fibre orientation at the interface has a negligible influence if the CFRP component has a multi-axial layer structure. On the other hand, it could be because all CFRP specimens were manufactured under the same process conditions, so their interlaminar shear strength does not differ significantly. Although the fibre direction at the boundary layer does not significantly influence the determined shear strength in the multiaxial layer structure, significant differences in the appearance of the fracture surfaces are observed. The fracture surfaces show that the 0°-specimens fail between the symmetrical 0°-layers (Figure 21a). In comparison, the 90°-specimens tend to fail in the 45° layer (Figure 21b). This indicates that the force is introduced into the interface between the first layer and the adjacent 45° layer.

3.2.3. Comparison of CFRP- and hybrid specimens

The results of CFRP and hybrid specimens (Figures 17b and 20a) were compared with the ANOVA analysis. The resulting P-value for 90°-specimens was 0.046, indicating significant differences between the tested groups. Therefore, the average shear strength determined for the hybrid 90°-specimens $\tau = 55.8$ MPa is significantly higher than that of CFRP 90°-specimens $\tau = 50.1$ MPa. Although the hybrid 90°-specimens still exhibit cohesive failure in the CFRP part, it can be seen from the fracture surfaces (Figure 18b) that the hybrid 90°-

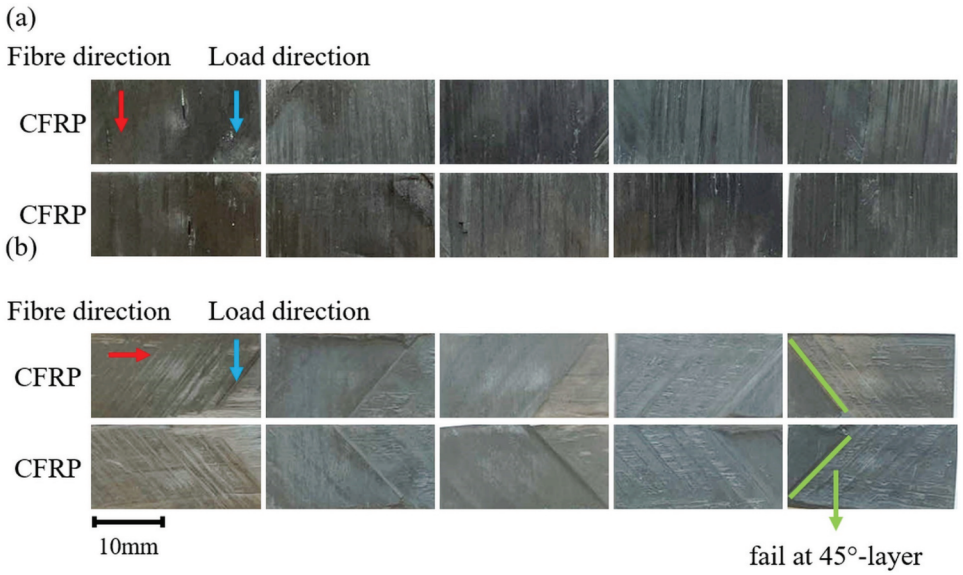

Figure 21. Fracture surfaces of CFRP specimens with multiaxial layer structure, (a) 0°-specimens, (b) 90°-specimens with the illustration of fibre direction of the first prepreg layer and load direction.

specimens exhibit failure at the 0° layer instead of the 45° layer, as is the case for the CFRP 90°-specimens. This could be caused by better joint strength at the interface of the hybrid specimens than between the prepreg layers in CFRP specimens, which allows the stress to be better transferred through the interface. In contrast to the 90°-specimens, all hybrid and CFRP 0°-specimens show failure in the first layer at the interface (Figures 18a and 21a). A P-value of 0.452 was calculated with the ANOVA analysis, meaning there are no significant differences in the determined shear strength between the hybrid 0°-specimens and the CFRP 0°-specimens. This again leads to the conclusion that the joint strength at the interface is better than that in the CFRP laminate, so the CFRP laminate fails earlier.

4. Summary and outlook

This study investigated the correlation between the adhesion properties in CFRP composite and the EN AW 6082-T6/CFRP hybrid specimens. The aluminium sheet was laser pretreated prior to hybridisation via prepreg pressing. The following factors were varied to analyse their influence on the adhesion properties of the hybrid joints: the number of prepreg layers, the layer structure of the CFRP laminate, laser scanning direction and fibre orientation at the interface. Shear edge tests were performed to assess the resulting shear strength. Furthermore, the fracture surfaces of the specimens

were characterised. All results were evaluated using ANOVA analysis. The main conclusions are summarised as follows:

- The stiffness of the joined parts influences the adhesion properties of the hybrid specimens. Increasing the number of prepreg layers increases the stiffness of the CFRP laminate, which enhances the force transmission during the test and influences the determined shear strength and the failure behaviour of the hybrid specimens.
- For hybrid specimens with a unidirectional layer structure, a higher shear strength can be achieved if the direction of force application is parallel to the fibre direction. However, this is not the case for hybrid specimens with a multiaxial layer structure in this study. It is assumed that the stiffness of the CFRP laminate can be significantly enhanced through the multiaxial layer structure so that the fibre direction at the interface only has a negligible influence.
- Apart from the increase in the number of prepreg layers, the laser scanning direction during the pretreatment also plays an important role in the resulting joint strength of the hybrid specimens. Depending on the scanning direction, the laser structures are realised in different orientations, influencing the failure behaviour. In this study, the specimens with SD1 show predominantly cohesive failure due to better mechanical interlocking. The determined shear strength for SD1 is almost the same as that of the CFRP specimens, which means that these specimens fail due to the failure of the CFRP laminate and that the joint strength at the interface is higher.
- Comparing the shear edge test results of hybrid specimens with those of CFRP specimens allows the conclusion that the determined shear strength of hybrid specimens, which are prone to cohesive failure, does not differ significantly from the interlaminar shear strength of the CFRP specimens. Therefore, the joint strength at the interface of such hybrid specimens is better than that in the CFRP laminate. In contrast, the shear strength determined for the hybrid specimens, which exhibit increased adhesive failure, exceeds the shear strength of the CFRP laminate.

This study shows that the stiffness in the FRP part influences the failure behaviour and, thus, the determined shear strength of the hybrid specimens. By analysing the shear strength in the FRP, it can be concluded whether the cohesive failure of hybrid specimens is due to the full utilisation of the interlaminar shear strength of CFRP or to a defect in the CFRP laminate. In the future, attempts should be made to further increase the inherent stiffness of the CFRP laminate and to produce hybrid specimens in which the aluminium surface is pretreated with scanning direction 1. This can be used to reveal

whether a higher shear strength of the hybrid joints or a different fracture surface can be achieved.

While the shear strength of the specimens in this work was characterised by the shear edge method to compare the results with the previous results,[20] further investigations need to be carried out using other test methods, such as tensile-shear- or short-beam tests, to investigate the influence of the test method on the joint strength of hybrid composites. Furthermore, Finite Element Simulation can be performed to investigate the stress state at the interface of the hybrid specimens with different layer structures or fibre orientations to characterise the dominant failure mechanisms.

Disclosure statement

No potential conflict of interest was reported by the author(s).

Funding

The research project is funded by the German Research Foundation [Deutsche Forschungsgemeinschaft] – project number [426499947] - "Energy-efficient manufacturing and mechanism-based corrosion fatigue characterization of laser-structured hybrid structures".

References

[1] European Environment Agency. EEA Greenhouse Gases - Data Viewer. https://www.eea.europa.eu/data-and-maps/data/data-viewers/greenhouse-gases-viewer. (accessed July 8, 2024).

[2] Joshi, A. M.; Ezzat, H.; Bucknor, N.; Verbrugge, M. Optimizing Battery Sizing and Vehicle Lightweighting for an Extended Range Electric Vehicle. *SAE Technical Paper Series, SAE International400 Commonwealth Drive*, 2011. DOI: 10.4271/2011-01-1078.

[3] Delogu, M.; Del Pero, F.; Pierini, M. Lightweight Design Solutions in the Automotive Field: Environmental Modelling Based on Fuel Reduction Value Applied to Diesel Turbocharged Vehicles. *Sustainability* 2016, *8*(11), 1167. DOI: 10.3390/su8111167.

[4] Del Pero, F.; Berzi, L.; Antonacci, A.; Delogu, M. Automotive Lightweight Design: Simulation Modeling of Mass-Related Consumption for Electric Vehicles. *Machines* 2020, *8*(3), 51. DOI: 10.3390/machines8030051.

[5] Hofer, J.; Wilhelm, E.; Schenler, W. Comparing the Mass, Energy, and Cost Effects of Lightweighting in Conventional and Electric Passenger Vehicles. *J. Sustain. Dev. Energy Water. Environ. Syst.* 2014, *2*(3), 284–295. DOI: 10.13044/j.sdewes.2014.02.0023.

[6] Bader, B.; Türck, E.; Vietor, T. Multi Material Design. A Current Overview of the Used Potential in Automotive Industries. *Technol. Econ. Funct. Lightweight Des.* 2019. DOI: 10.1007/978-3-662-58206-0_1.

[7] Kavitha, K.; Vijayan, R.; Sathishkumar, T. Fibre-Metal Laminates: A Review of Reinforcement and Formability Characteristics. *Mater. Today. Proc.* 2020, *22*, 601–605. DOI: 10.1016/j.matpr.2019.08.232.

[8] Zhu, G.; Sun, G.; Liu, Q.; Li, G.; Li, Q. On Crushing Characteristics of Different Configurations of Metal-Composites Hybrid Tubes. *Composite. Struct.* 2017, *175*, 58–69. DOI: 10.1016/j.compstruct.2017.04.072.

[9] Bachmann, J.; Hidalgo, C.; Bricout, S. Environmental Analysis of Innovative Sustainable Composites with Potential Use in Aviation Sector—A Life Cycle Assessment Review. *Sci. China Technol. Sci.* 2017, *60*(9), 1301–1317. DOI: 10.1007/s11431-016-9094-y.

[10] Min, J.; Hu, J.; Sun, C.; Wan, H.; Liao, P.; Teng, H.; Lin, J. Fabrication Processes of Metal-Fibre Reinforced Polymer Hybrid Components: A Review. *Adv. Compos. Hybrid. Mater.* 2022, *5*(2), 651–678. DOI: 10.1007/s42114-021-00393-z.

[11] Pramanik, A.; Basak, A. K.; Dong, Y.; Sarker, P. K.; Uddin, M. S.; Littlefair, G.; Dixit, A. R.; Chattopadhyaya, S. Joining of Carbon Fibre Reinforced Polymer (CFRP) Composites and Aluminium Alloys – a Review. *Compos. Part A. Appl. Sci. Manuf.* 2017, *101*, 1–29. DOI: 10.1016/j.compositesa.2017.06.007.

[12] Santos, D. D.; Carbas, R.; Marques, E.; Da Silva, L. Reinforcement of CFRP Joints with Fibre Metal Laminates and Additional Adhesive Layers. *Compos. Part B. Eng.* 2019, *165*, 386–396. DOI: 10.1016/j.compositesb.2019.01.096.

[13] Jeevi, G.; Nayak, S. K.; Abdul Kader, M. Review on Adhesive Joints and Their Application in Hybrid Composite Structures. *J. Adhes. Sci. Technol.* 2019, *33*(14), 1497–1520. DOI: 10.1080/01694243.2018.1543528.

[14] Voswinkel, D.; Kloidt, D.; Grydin, O.; Schaper, M. Time Efficient Laser Modification of Steel Surfaces for Advanced Bonding in Hybrid Materials. *Prod. Eng. Res. Devel.* 2021, *15*(2), 263–270. DOI: 10.1007/s11740-020-01006-2.

[15] Freund, J.; Löbbecke, M.; Delp, A.; Walther, F.; Wu, S.; Tröster, T.; Haubrich, J. Relationship Between Laser-Generated Micro- and Nanostructures and the Long-Term Stability of Bonded Epoxy-Aluminum Joints. *J. Adhes.* 2024, *100*(6), 395–425. DOI: 10.1080/00218464.2023.2223475.

[16] Akman, E.; Bora, M. Ö.; Çoban, O.; Oztoprak, B. G. Laser-Induced Groove Optimization for Al/CFRP Adhesive Joint Strength. *Int. J. Adhes. Adhes.* 2021, *107*, 102830. DOI: 10.1016/j.ijadhadh.2021.102830.

[17] Li, H.; Liu, H.; Li, S.; Zhao, Q.; Qin, X. Influence of High Pulse Fluence Infrared Laser Surface Pretreatment Parameters on the Mechanical Properties of CFRP/Aluminium Alloy Adhesive Joints. *J. Adhes.* 2023, *99*(4), 584–605. DOI: 10.1080/00218464.2022.2027242.

[18] Reitz, V.; Meinhard, D.; Ruck, S.; Riegel, H.; Knoblauch, V. A Comparison of IR- and UV-Laser Pretreatment to Increase the Bonding Strength of Adhesively Joined Aluminum/CFRP Components. *Compos. Part A. Appl. Sci. Manuf.* 2017, *96*, 18–27. DOI: 10.1016/j.compositesa.2017.02.014.

[19] Koch, S. F.; Barfuss, D.; Bobbert, M.; Groß, L.; Grützner, R.; Riemer, M.; Stefaniak, D.; Wang, Z. Intrinsic Hybrid Composites for Lightweight Structures: New Process Chain Approaches. *AMR.* 2016, *1140*, 239–246. DOI: 10.4028/www.scientific.net/AMR.1140.239.

[20] Wu, S.; Delp, A.; Freund, J.; Walther, F.; Haubrich, J.; Löbbecke, M.; Tröster, T. Adhesion Properties of the Hybrid System Made of Laser-Structured Aluminium EN AW 6082 and CFRP by Co-Bonding-Pressing Process. *The J. Adhes.* 2023, *100*(8), 639–667. DOI: 10.1080/00218464.2023.2245758.

[21] Weidenmann, K. A.; Baumgärtner, L.; Haspel, B. The Edge Shear Test - an Alternative Testing Method for the Determination of the Interlaminar Shear Strength in Composite Materials. *MSF* 2015, *825-826*, 806–813. DOI: 10.4028/www.scientific.net/MSF.825-826.806.

[22] Kadioglu, F.; Puskul, H. Effects of Different Fibre Orientations on the Shear Strength Performance of Composite Adhesive Joints. *World. Acad. Sci. Eng. Technol. Int. J. Mater. Metallurgical Eng.* 2016, *10*, 65–68. DOI: 10.5281/zenodo.1338740.

[23] Naresh, K.; Shankar, K.; Velmurugan, R. Effect of Fibre Orientation on Carbon/Epoxy and Glass/Epoxy Composites Subjected to Shear and Bending. *SSP* 2017, *267*, 103–108. DOI: 10.4028/www.scientific.net/SSP.267.103.

[24] Zinn, C.; Bobbert, M.; Dammann, C.; Wang, Z.; Tröster, T.; Mahnken, R.; Meschut, G.; Schaper, M. Shear Strength and Failure Behaviour of Laser Nano-Structured and Conventionally Pre-Treated Interfaces in Intrinsically Manufactured CFRP-Steel Hybrids. *Compos. Part B. Eng.* 2018, *151*, 173–185. DOI: 10.1016/j.compositesb.2018.05.030.

[25] Aydın, M. D. 3-D Nonlinear Stress Analysis on Adhesively Bonded Single Lap Composite Joints with Different Ply Stacking Sequences. *J. Adhes.* 2008, *84*(1), 15–36. DOI: 10.1080/00218460801888359.

[26] Kowatz, J.; Teutenberg, D.; Meschut, G. Experimental Failure Analysis of Adhesively Bonded Steel/CFRP Joints Under Quasi-Static and Cyclic Tensile-Shear and Peel Loading. *Int. J. Adhes. Adhes.* 2021, *107*, 102851. DOI: 10.1016/j.ijadhadh.2021.102851.

[27] Larson, M. G. Analysis of Variance. *Circulation* 2008, *117*(1), 115–121. DOI: 10.1161/CIRCULATIONAHA.107.654335.

[28] Kanani, A. Y.; Kanani, Y.; Hughes, X. D. J.; Ye, J.; Hou, X. Fracture Mechanisms of Hybrid Adhesive Bonded Joints: Effects of the Stiffness of Constituents. *Int. J. Adhes. Adhes.* 2020, *102*, 102649. DOI: 10.1016/j.ijadhadh.2020.102649.

[29] Pereira, A. M.; Ferreira, J. M.; Antunes, F. V.; Bártolo, P. J. Analysis of Manufacturing Parameters on the Shear Strength of Aluminium Adhesive Single-Lap Joints. *J. Mater. Process. Technol.* 2010, *210*(4), 610–617. DOI: 10.1016/j.jmatprotec.2009.11.006.

[30] de Morais, A. B.; Pereira, A. B.; Teixeira, J. P.; Cavaleiro, N. C. Strength of Epoxy Adhesive-Bonded Stainless-Steel Joints. *Int. J. Adhes. Adhes.* 2007, *27*(8), 679–686. DOI: 10.1016/j.ijadhadh.2007.02.002.

[31] Ostapiuk, M.; Bieniaś, J. Fracture Analysis and Shear Strength of Aluminum/CFRP and GFRP Adhesive Joint in Fibre Metal Laminates. *Materials* 2019, *13*(1), 7. DOI: 10.3390/ma13010007.

[32] Grefe, H.; Kandula, M. W.; Dilger, K. Influence of the Fibre Orientation on the Lap Shear Strength and Fracture Behaviour of Adhesively Bonded Composite Metal Joints at High Strain Rates. *Int. J. Adhes. Adhes.* 2020, *97*, 102486. DOI: 10.1016/j.ijadhadh.2019.102486.

[33] Kupski, J.; Teixeira de Freitas, S.; Zarouchas, D.; Camanho, P. P.; Benedictus, R. Composite Layup Effect on the Failure Mechanism of Single Lap Bonded Joints. *Composite. Struct.* 2019, *217*, 14–26. DOI: 10.1016/j.compstruct.2019.02.093.

[34] Purimpat, S.; Jérôme, R.; Shahram, A. Effect of Fibre Angle Orientation on a Laminated Composite Single-Lap Adhesive Joint. *Adv. Compo. Mater.* 2013, *22*(3), 139–149. DOI: 10.1080/09243046.2013.782805.